

UKAEA-CCFE-PR(23)109

Xu Yang, Yueqiang Liu, Wei Xu, Yuling He, Guoliang
Xia

Effect of negative triangularity on tearing mode stability in tokamak plasmas

Enquiries about copyright and reproduction should in the first instance be addressed to the UKAEA Publications Officer, Culham Science Centre, Building K1/O/83 Abingdon, Oxfordshire, OX14 3DB, UK. The United Kingdom Atomic Energy Authority is the copyright holder.

The contents of this document and all other UKAEA Preprints, Reports and Conference Papers are available to view online free at scientific-publications.ukaea.uk/

Effect of negative triangularity on tearing mode stability in tokamak plasmas

Xu Yang, Yueqiang Liu, Wei Xu, Yuling He, Guoliang Xia

Effect of negative triangularity on tearing mode stability in tokamak plasmas

Xu Yang^{1,*}, Yueqiang Liu², Wei Xu³, Yuling He^{4,*}, Guoliang Xia⁵

¹ Department of Physics, and Chongqing Key Laboratory of Intelligent Perception and BlockChain Technology, Chongqing Technology and Business University, Chongqing 400067, China

² General Atomics, PO Box 85608, San Diego, CA 92186-5608, USA

³ National Research Base of Intelligent Manufacturing Service, Chongqing Technology and Business University, Chongqing 400067, China

⁴ Guangdong Provincial Key Laboratory of Quantum Engineering and Quantum Materials, GPETR Center for Quantum Precision Measurement, SPTE, South China Normal University, Guangzhou 510006, China

⁵ CCFE, Culham Science Centre, Abingdon OX14 3DB, United Kingdom

E-mail: yangxu@ctbu.edu.cn; heyl@m.scnu.edu.cn

Abstract

The influence of negative plasma triangularity on the $n=1$ (n is the toroidal mode number) tearing mode (TM) stability has been numerically investigated, with results compared to that of the positive triangularity counterpart. By matching the safety factor profile for a series of toroidal equilibria, several important plasma parameters, including the triangularity, the plasma equilibrium pressure, the plasma resistivity as well as the toroidal rotation, have been varied. As a key finding, the TM is generally more unstable in the negative triangularity plasmas as compared to the positive triangularity counterpart. The fundamental reason for this difference is the lack of favorable average curvature stabilization in negative triangularity configurations. Direct comparison of the Mercier index corroborates this conclusion. The plasma toroidal flow generally stabilizes the TM in plasmas with both negative and positive triangularities. The flow stabilization is however weaker in the case of negative triangularity with finite plasma pressure.

1. Introduction

The tearing mode (TM) is one of the most important macroscopic magnetohydrodynamics (MHD) instabilities, that leads to reconnection of the magnetic field lines (near the location of the instability) [1-3], degradation of the plasma energy confinement [4-6], and potentially plasma major disruption [7-9]. Large magnetic islands, induced by the TM or its neoclassical counterpart, limit the plasma equilibrium pressure in terms of the normalized values $\beta = 2\mu_0 \langle P \rangle / B_0^2$ and $\beta_N = \beta[\%]a[m]B_0[T]/I_p[MA]$, where β is the ratio of the volume averaged plasma pressure $\langle P \rangle$ to the magnetic pressure, B_0 the on-axis toroidal magnetic field strength, a the plasma minor radius and I_p the plasma total current. On the other hand, it is well known that finite β , in association with the finite pressure gradient across the mode rational surface, stabilizes the TM via the favorable average curvature effect (the so-called GGJ-effect [10]) in tokamak geometry. As interesting consequences, the GGJ-effect can introduce finite frequency to the mode even in a static plasma [11-13]. A rotating TM (in an initially static plasma) in turn generates net electromagnetic torque and drives plasma flow [12]. Furthermore, the GGJ-effect induced energy dissipation was also found responsible for a strong stabilization of the resistive-plasma resistive wall mode (RP-RWM) [12]. Finally, as β_N approaches the so-called no-wall Troyon limit, the plasma equilibrium pressure can be destabilizing to the TM, by coupling the instability to the ideal kink mode [12].

The boundary shape of the plasma poloidal cross-section plays important roles in the discharge performance in tokamak fusion devices [14-16]. Conventionally, a ‘D’-shaped plasma with positive triangularity (PT) has been shown to be favorable for reducing the energy transport and increasing the β_N limit [17, 18]. Recent experiments, however, have shown that a reversed ‘D’-shape with negative triangularity (NT) can also help reduce the turbulence-induced energy transport as well and reach a global

confinement comparable to the H-mode regime of PT-plasmas [19-21]. Absence of edge localized modes in NT-plasmas is another advantage [22]. Because of the aforementioned (and other) interesting features associated with the NT-configuration, operation with reversed ‘D’-shape for the plasma boundary is becoming an attractive fusion concept during recent years [22-29].

In this study, we investigate the effect of negative triangularity of the plasma shape on the TM stability through toroidal modeling, and compare with that for the positive triangularity counterpart. The NT-effect on tearing mode has so far not been systematically investigated in theory and modeling, much less in terms of achieving physics understanding which is the primary focus of the present work. A recent study [29] has partially considered the NT-effect on the TM, but in the context of reversed magnetic shear plasma scenarios (i.e. on the so-called double tearing mode). Our results here reveal the key physics difference introduced by the NT-shape, as compared to the PT-shape, that affects the TM stability. More specifically, we find that the NT-shape substantially reduces the favorable average curvature stabilization, leading to a more robust TM instability in tokamak plasmas. As for the toroidal modeling tool, we employ the MARS-F code [30] to solve the resistive MHD eigenvalue problem without ordering assumptions.

The paper is organized as follows. Section 2 describes a series of numerical plasma equilibria that we construct in full toroidal geometry, that covers plasma boundary shapes ranging from negative to positive triangularity. A key feature of these equilibria is that the safety factor profile is fixed to be nearly identical while varying the plasma triangularity. Section 3 reports detailed modeling results on the TM stability as well as discussions on the underlying physics effects associated with the GGJ-stabilization and the Shafranov shift. Section 4 summarizes the results.

2. Plasma equilibria

In this study, we adopt semi-analytic equilibria in toroidal tokamak geometry, without referencing to specific devices. These equilibria are constructed for physics understanding of the NT-shape on the TM stability, and appropriate constraints on the equilibria are employed to facilitate achieving the goal.

We consider lower single null divertor-like plasmas, with the boundary shape specified in the (R, Z) coordinates on the poloidal plane [31] and normalized by the plasma major radius R_0 (which is assumed to be 3 m)

$$R(\theta) = 1 + \varepsilon \cos(\theta + \delta \sin(\theta)) \quad (2.1)$$

$$Z(\theta) = \varepsilon \kappa \sin(\theta) - b \exp \left[- \left(\left| \theta + \frac{\pi}{2} \right| / c \right)^{3/2} \right] \quad (2.2)$$

where the parameters ε , δ , κ define the inverse aspect ratio of the plasma, the triangularity and elongation of the plasma boundary shape. In order to construct a lower single null plasma configuration, we specify, $b=0.08$ and $c=0.5$. The parameters ε and κ are fixed at $1/3$ and 1.5 , respectively, in this study. The key parameter that we vary is the boundary triangularity δ . Figure 1(a) shows examples of the constructed plasma boundary shape while varying δ from -0.3 to 0.3 . As will be reported later, choosing this range of δ well covers the physics regime (the GGJ-regime) of interest here - the GGJ-effect disappears when $\delta < -0.3$ for the series of equilibria considered.

An important consideration in studying the TM is the safety factor profile q , which is known to strongly affect the mode stability via the radial location of the associated rational surfaces as well as the local magnetic shear. In order to eliminate the effect of the q -profile on the TM stability while scanning plasma triangularity, we tune the plasma current density profile (which is one of the input data of our fixed-boundary

equilibrium solver [32]) to ensure nearly identical safety factor profiles, as shown in Fig. 1(b). Note that the safety factor is the output of the Grad-Shafranov solver here, and is numerically self-consistently computed. To avoid the internal kink instability, we fixed the on-axis safety factor at $q_0 = 1.2$. The $q=2$ rational surface, which plays important roles in the $n=1$ TM in this study, is located near $s=0.95$ where s labels the plasma radial coordinate. Note that we also limit the edge safety factor below 3 to focus on the $m=2/n=1$ resonant component (m is the poloidal harmonic number).

We also scan the normalized plasma pressure by varying the overall amplitude while fixing the radial profile of the equilibrium pressure to an analytic form $P=P_0(1-s^2)^2$. For the TM stability in this study, what matter most are the local pressure and pressure gradient at the $q=2$ surface.

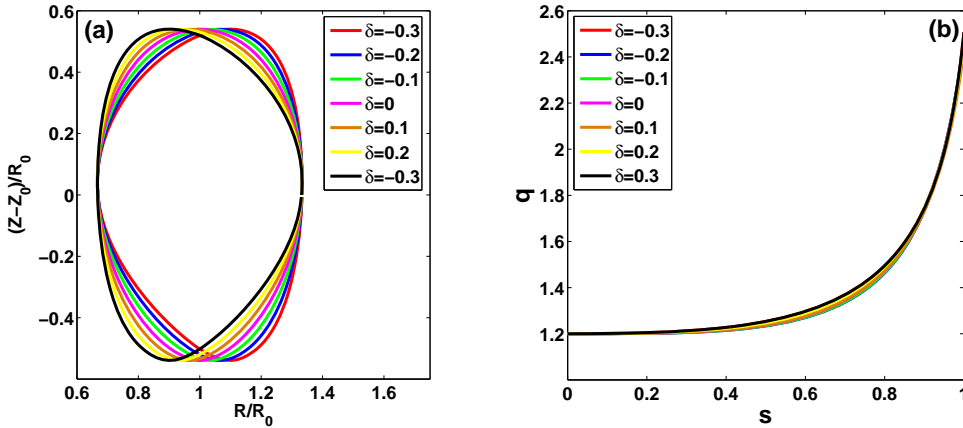


Figure 1. The (a) plasma boundary shapes (normalized by the major radius R_0), and (b) radial profiles of the safety factor q , considered in this study.

3. Modeling results

We focus on investigating the effect of negative triangularity on the stability of the $n=1$ TM at the $q=2$ surface. Three plasma equilibrium parameters are of our primary concern while scanning the triangularity, i.e., the plasma pressure (β_N), resistivity

(Lundquist number S), and the plasma toroidal rotation. We start by reporting the modeling results for plasmas with vanishing flow.

Figures 2 and 3 report the MARS-F computed TM growth rate and mode frequency, respectively, for a series of equilibria with different triangularity while performing scans in 2D parameter space of β_N and S . The range for β_N is 0–1.77. The upper bound here is chosen to be reasonably below the Troyon no-wall limit for the onset of the $n=1$ ideal kink instability. At $\beta_N > 1.77$, we find that the TM eigenfunction becomes more global and starts to resemble that of an ideal kink. The range for the Lundquist number S is chosen to be $2 \times 10^6 - 10^{10}$. This covers the values for the Lundquist number in typical tokamak discharges. Note that the Lundquist number is defined as $S = \tau_R / \tau_A$, where $\tau_R = \mu_0 a^2 / \eta$ (η being the plasma resistivity and μ_0 vacuum permeability) is the resistive decay time of the plasma current and $\tau_A = R_0 \sqrt{\mu_0 \rho_0} / B_0$ is the toroidal Alfvén time (R_0 and a are the plasma major and minor radii, respectively).

Figure 2 shows that the TM growth rate generally decreases with increasing triangularity (from the negative to positive values). In fact with $\delta \geq 0$ and sufficiently high Lundquist number ($S \geq 10^8$), stable TM is computed in certain parameter spaces. At a given triangularity, the TM growth rate decreases with increasing Lundquist number. This is expected since the TM is driven by the plasma resistivity. It is on the other hand interesting to observe the different dependence of the mode stability on β_N between the NT- and PT-plasmas. For a NT-equilibrium (Fig. 2(a-c)), higher plasma pressure drives more unstable TM. The trend is however reversed for the PT-counterpart (Fig. 2(e-f)). The finite-pressure induced TM stabilization in PT-plasmas is associated with the GGJ-effect. The lack of such stabilization in the NT-plasmas indicates a weak GGJ-effect – an important finding of this study which will be further elaborated later on.

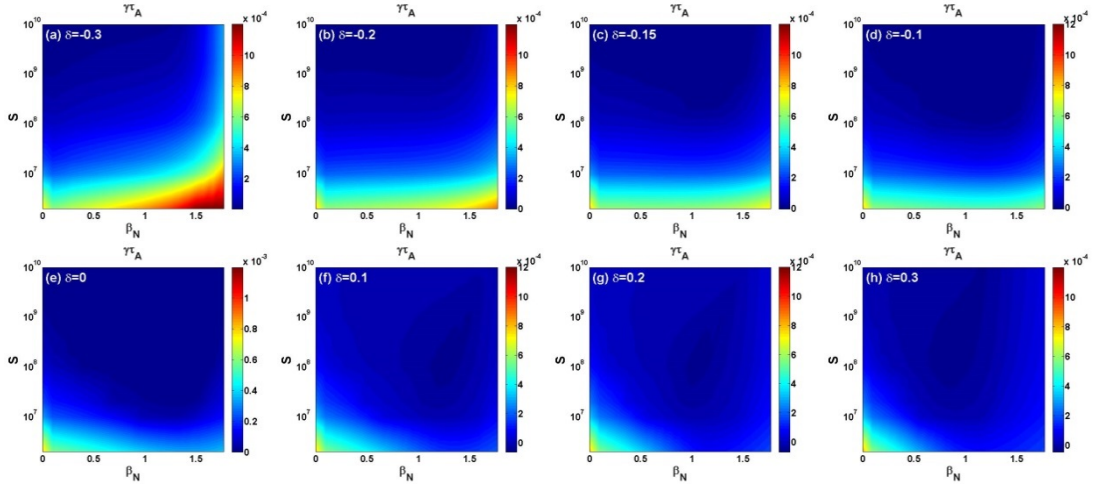


Figure 2. Plotted are the growth rate of the mode from negative to positive triangularity, while varying the β_N and the Lundquist number S .

The presence of GGJ-stabilization often results in finite mode frequency (even in the absence of plasma rotation). This is indeed the case for the PT-plasmas as shown in Fig. 3. As δ is progressively increased from the negative to positive values, an “island” of finite-frequency region appears in the (β_N, S) domain. This “island” emerges from the high- S end for plasmas with weak negative triangularity (Fig. 3(c-d)), and becomes as a prominent feature for PT-plasmas (Fig. 3(e-h)). Presence of finite mode frequency is a clear indication of the GGJ-effect on the TM (at intermediate finite plasma pressure). Note that the regions with prominent frequency-islands also correspond to the “meta-stable” regions for the TM stability shown in Fig. 2. Absence of such “islands” for equilibria with strongly negative triangularity (Fig. 3(a-b)) indicates lack of GGJ-stabilization independent of the plasma pressure and resistivity.

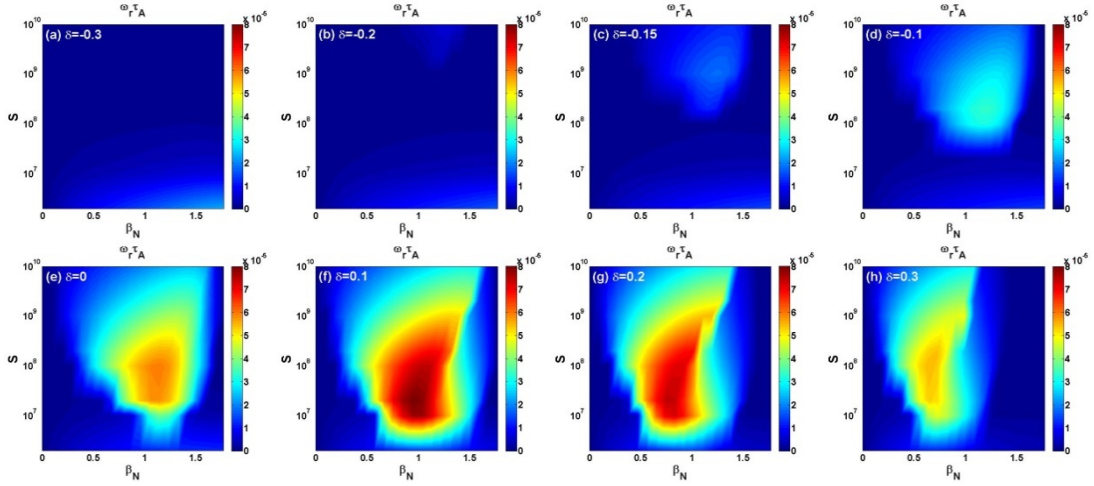


Figure 3. Plotted are the real frequency of the mode from negative to positive triangularity, while varying the β_N and the Lundquist number S .

As direct evidence for the presence or absence of the GGJ-effect, Fig. 4(a-b) shows the ideal (D_I) and resistive (D_R) Mercier indices evaluated at the $q=2$ surface, for the equilibria considered here. These equilibrium quantities are presented in the 2D parameter space of (β_N, δ) . Note that $D_I=1/4$ corresponds to the case of vanishing plasma pressure where no GGJ-effect is present for all triangularity values. This quantity increases with both β_N and δ . We mention that D_I exceeding unity corresponds to the ideal kink stability limit [33], which has evidently not been accessed for our series of equilibria.

The computed Mercier index D_R is of small negative values for the PT-plasmas at sufficiently high pressure (Fig. 4(b)). A negative D_R is directly associated with the GGJ-stabilization, which is proportional to D_R [10]. This quantity is however close to 0 for NT-equilibria, for a large range of β_N values. Figure 4(b) thus reveals the reason for the robust TM instability computed for the NT-plasmas as reported in Fig. 2.

Since the Shafranov shift is also known to affect the MHD instability, we evaluate this quantity as well for our equilibria, with results plotted in Fig. 4(c). Here, we define the Shafranov shift as the radial distance of the magnetic axis (R_{axis}) with

respect to the geometrical center (R_0) of the plasma. The normalized quantity reported in Fig. 4(c) is thus $\Delta/R_0=(R_{\text{axis}}-R_0)/R_0$. Figure 4(c) shows that the plasma pressure enhances the Shafranov shift, as expected. More importantly, increasing the plasma triangularity (from negative to positive values) results in reduced Shafranov shift. Since the Shafranov shift typically stabilizes MHD instabilities (in particular ballooning type of modes), the computed destabilization of the TM in the NT-plasmas (with large Shafranov shift) is not due to this effect. We thus conclude that the lack of the GGJ-stabilization is the main reason for the more unstable TM in NT-plasmas.

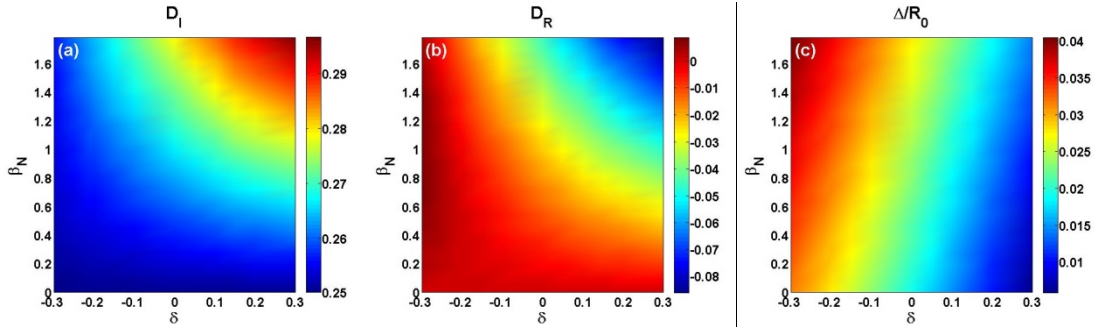


Figure 4. The (a) ideal and (b) resistive Mercier index at the $q=2$ surface, and (c) normalized Shafranov shift, while varying the β_N and the triangularity δ .

We have performed denser scan of the plasma triangularity than that reported in Figs. 2 and 3. Figure 5 show two representative examples of the computed TM growth rate versus δ . One case ($\beta_N=0$ and $S=10^8$) is chosen from the top-left corner of the 2D parameter domain in Fig. 2, where the mode growth rate is too small to be clearly compared in the 2D plots. The other case ($\beta_N=0.5$ and $S=2 \times 10^6$) is chosen near the bottom-middle region from Fig. 2, where the instability remains relatively strong for all triangularity values. Note that we are also comparing two cases here with ($\beta_N=0.5$) and without ($\beta_N=0$) the GGJ-effect. The presence of the favorable average curvature effect evidently results in substantial stabilization of the TM as we increase the plasma triangularity from negative to positive values. The slight stabilization (with *decreasing* δ) of the mode for the case of vanishing equilibrium pressure (thus no

GGJ-stabilization) may be due to the increase of the Shafranov shift as shown in Fig. 4(c).

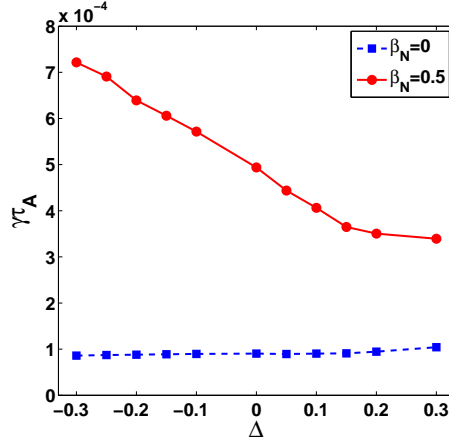


Figure 5. The normalized growth rate of the $n=1$ tearing mode versus the plasma boundary triangularity δ , computed assuming (a) $\beta_N=0$ and $S=10^8$, and (b) $\beta_N=0.5$ and $S=2 \times 10^6$.

As a final study of this work, we consider the negative triangularity effect on the TM stability in toroidally rotating plasmas. We consider two flow models, i.e., a uniform rotation along the plasma minor radius ($\Omega=\Omega_0$) and a sheared rotation ($\Omega=\Omega_0(1-s^2)$). The modeling results are reported in Fig. 6, again for the two cases of ($\beta_N=0$, $S=10^8$) and ($\beta_N=0.5$, $S=2 \times 10^6$) as in Fig. 5. Note that, with the same on-axis rotation frequency Ω_0 , the plasma rotation at the $q=2$ rational surface is much slower for the sheared flow case, as compared to the uniform flow. This motivates our choice of larger ranges for Ω_0 for sheared flow cases, in particular for the case with finite equilibrium pressure as shown in Fig. 6(d,h).

In general, we find that the plasma toroidal rotation reduces the TM growth rate independent of the flow models. For the $\beta_N=0$ case (Fig. 6(a-b)), the degree of stabilization is similar between NT- and PT-plasmas. At finite equilibrium pressure (Fig. 6(c-d)), however, the TM growth rate is less affected by plasma rotation for

NT-equilibria. In all cases, the mode frequency roughly linearly increases with the plasma local rotation frequency at the $q=2$ surface (Fig. 6(e-h)), as expected.

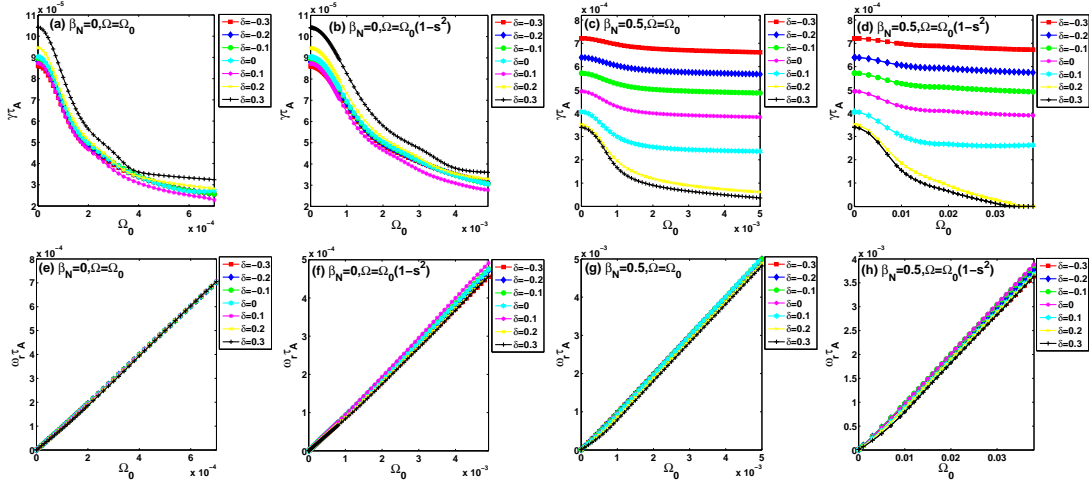


Figure 6. The computed normalized (a-d) growth rate, and (e-h) real frequency of the $n=1$ tearing mode, assuming (a, b, e, f) $\beta_N=0$ and $S=10^8$, and (c, d, g, h) $\beta_N=0.5$ and $S=2 \times 10^6$, while varying the plasma toroidal rotation frequency. Assumed are two rotation profile models, with (a, c, e, g) a uniform rotation profile $\Omega=\Omega_0$ along the plasma minor radius and (b, d, f, h) a sheared rotation profile $\Omega=\Omega_0(1-s^2)$.

4. Conclusion and discussion

We have numerically investigated the influence of (negative) plasma triangularity on the $n=1$ TM in this work. By matching the safety factor profile for a series of toroidal equilibria, we scan several plasma parameters including the triangularity, the plasma equilibrium pressure, the plasma resistivity as well as the toroidal rotation.

As a key finding, the TM is generally more unstable in the NT-plasmas as compared to the PT-counterpart. The fundamental reason for this difference is the lack of favorable average curvature stabilization in NT-plasmas, at least for the TM. Comparison of the Mercier index corroborates this conclusion. The Shafranov shift, which tends to be larger for the NT-equilibria, does not help to stabilize the mode

except perhaps for the peculiar case of vanishing equilibrium pressure.

The plasma toroidal flow generally stabilizes the TM in plasmas with both negative and positive triangularities. For the cases of vanishing equilibrium pressure, the degree of stabilization is similar between the NT- and PT-plasmas. For finite pressure cases, however, we find that the flow stabilization is weaker for the NT-plasma.

The above findings, in particular the physics understanding revealed by the numerical modeling, can be useful for interpreting experimental results in NT-plasmas. On the other hand, we point out that not all physics effects have been included in our present study, such as the neoclassical effects (NTM) and the non-linear effects, effects beyond standard single-fluid MHD model (e.g. anisotropic thermal transport effect which we will study in the near future). Some of these effects may also significantly affect the TM behavior in negative-triangularity plasmas.

Acknowledgements.

This work was supported by the National Natural Science Foundation of China (Grant Nos. 11905022, 11905067 and 12075053), Chongqing Basic Research and Frontier Exploration Project in 2019 (Chongqing Natural Science Foundation, Grant No. cstc2019jcyj-msxmX0567), the Science and Technology Research Program of Chongqing Municipal Education Commission (Grant Nos. KJQN202200819), and the project of Chongqing Technology and Business University (Grant No. 1952039 and 2056017). The work was also supported by the U.S. DoE Office of Science under Contract Nos. DE-FG02-95ER54309 and DE-FC02-04ER54698. This report was prepared as an account of work sponsored by an agency of the United States Government. Neither the United States Government nor any agency thereof, nor any of their employees, makes any warranty, express or implied, or assumes any legal liability or responsibility for the accuracy, completeness, or usefulness of any information, apparatus, product, or process disclosed, or represents that its use would not infringe privately owned rights. Reference herein to any specific commercial product, process, or service by trade name, trademark, manufacturer, or otherwise, does not necessarily constitute or imply its endorsement, recommendation, or favoring by the United States Government or any agency thereof. The views and opinions of authors expressed herein do not necessarily state or reflect those of the United States Government or any agency thereof.

References

- [1] Furth H P *et al* 1963 *Phys. Fluids* **6** 459-484
- [2] Chu M S *et al* 2002 *Phys. Plasmas* **9** 4584
- [3] Huang W *et al* 2021 *Nucl. Fusion* **61** 036047
- [4] Nishimura Y *et al* 1997 *Phys. Plasmas* **4** 2365
- [5] La Haye R J 2006 *Phys. Plasmas* **13** 055501
- [6] Hu Q *et al* 2019 *Nucl. Fusion* **59** 016005
- [7] Kikuchi M *et al* 2012 *Reviews of Modern Physics* **84** 1807-1854
- [8] Wei L *et al* 2016 *Nucl. Fusion* **56** 106015
- [9] Huang W 2022 *Plasma Phys. Control. Fusion* **64** 055023
- [10] Glasser A H *et al* 1976 *Phys. Fluids* **19** 567
- [11] Liu Y *et al* 2012 *Phys. Plasmas* **19** 072509
- [12] Hao G Z *et al* 2014 *Phys. Plasmas* **21** 012503
- [13] Liu T *et al* 2017 *Plasma Phys. Control. Fusion* **59** 065009
- [14] Moret J M *et al* 1997 *Phys. Rev. Lett.* **79** 2057
- [15] Fontana M *et al* 2018 *Nucl. Fusion* **58** 024002
- [16] Yang X *et al* 2022 *Nucl. Fusion* **62** 016013
- [17] Yamazaki K 1980 *Jpn. J. Appl. Phys.* **19** 963
- [18] Wilson H R *et al* 2002 *Phys. Plasmas* **9** 1277
- [19] Camenen Y *et al* 2007 *Nucl. Fusion* **47** 510-516
- [20] Kirneva N A *et al* 2012 *Plasma Phys. Control. Fusion* **54** 015011
- [21] Marinoni A *et al* 2021 *Reviews of Modern Plasma Physics* **5:6**
- [22] Austin M E *et al* 2019 *Phys. Rev. Lett.* **122** 115001
- [23] Sauter O *et al* 2014 *Phys. Plasmas* **21** 055906
- [24] Ren J *et al* 2016 *Plasma Phys. Control. Fusion* **58** 115009
- [25] Ren J *et al* 2018 *Nucl. Fusion* **58** 126017
- [26] Xue L *et al* 2019 *Fusion Engineering and Design* **143** 48-58
- [27] Zhou L *et al* 2021 *Plasma Phys. Control. Fusion* **63** 065007
- [28] Abate D *et al* 2020 *Plasma Phys. Control. Fusion* **62** 085001
- [29] Wang H Y *et al* 2022 *Plasma Phys. Control. Fusion* **64** 085005
- [30] Liu Y *et al* 2000 *Phys. Plasmas* **7** 3681-3690
- [31] Liu Y *et al* 2020 *Plasma Phys. Control. Fusion* **62** 045001
- [32] Lütjens H *et al* 1992 *Comput. Phys. Commun.* **69** 287-298
- [33] Brennan D P *et al* 2002 *Phys. Plasmas* **9** 2998